ARTICLES

Raman Characterization and Tunable Growth of Double-Wall Carbon Nanotubes

Lijie Ci,† Zhenping Zhou, Xiaoqin Yan, Dongfang Liu, Huajun Yuan, Li Song, Jianxiong Wang, Yan Gao, Jianjun Zhou, Weiya Zhou, Gang Wang, and Sishen Xie*

Institute of Physics, Center for Condensed Matter Physics, Chinese Academy of Science, Beijing 100080, P. R. China

Received: July 12, 2002; In Final Form: June 2, 2003

Double-wall carbon nanotubes (DWCNTs) were synthesized by pyrolyzing C_2H_2 on the sulfur-promoted floating iron catalyst. Similar to that of SWCNTs, Raman spectra of DWCNTs display two "fingerprint" features of the radial breathing mode (RBM) at the lower frequency range and the splitting tangential mode (TM). However, RBM frequencies of DWCNTs take a wider range and display much richer peaks than those of SWCNTs. The possible match of the inner tubes and the outer tubes according to the RBM bands was assigned, and different chirality types were discussed according to the diameter and chirality dependence of resonant Raman vibration. By changing experimental conditions, we can tunably grow different DWCNTs with various diameter distributions.

1. Introduction

Since Iijima's discovery of carbon nanotubes,[1] selective production of specific types of nanotubes, such as single-wall carbon nanotubes (SWCNTs),[2] has become one of the principal goals in this field. Double-wall carbon nanotubes (DWCNTs), which consist of two concentric cylindrical graphene layers, have been attracting increasing interest as the simplest member of the multiwall carbon nanotubes (MWCNTs) in recent years. Theoretical study indicated that the structure of a DWCNT could be any chirality pairs of inner and outer layers,[3] which suggested that DWCNTs have more complex properties than that of SWCNTs. It is also revealed that the band structure of a DWCNT depends on the combination of the configurations of the inner and outer tubes,[4] and their stability depends only on their interlayer spacing.[3] Studies on the interlayer coupling of the inner and the outer layers can provide a basic understanding of the interlayer interaction modes of MWCNTs. For example, the interlayer coupling may periodically open and close four pseudo-gaps near Fermi level in a metallic DWCNT, which is unique and does not occur in single-wall carbon nanotubes (SWCNTs).[5] Therefore, the selective production of a pure DWCNT sample is highly desired. In our previous paper,[6] we developed a floating catalyst CVD method to selectively produce DWCNTs in bulk. In this paper, we will report the Raman scattering results of the DWCNTs.

Raman scattering is the useful technique to study the one-dimensional properties of carbon nanotubes, since it can probe both the phonon spectrum and the electronic structure. Previous Raman scattering investigation mostly focused on the SWCNTs in the theoretical work and experimental researches.[7−9] Studies on the Raman spectra of the DWCNTs were scarce due to the difficulty of their selective production. Bandow et al.[10] first investigated the Raman spectra of DWCNTs prepared by heating fullerene-encapsulated SWCNTs at a high temperature of 1200 °C. They observed two groups of radial breathing mode (RBM) bands that respectively originate from the outer parent tubes and the inner tubes. However, Raman spectra of DWCNTs recently prepared by the arc discharge method did not show any "fingerprint" modes.[11] In this paper, we will demonstrate that DWCNTs prepared by the CVD method can be well characterized by the Raman scattering technique.

Carbon nanotubes have some novel properties associated with their different structure. Therefore, selectively growing different types of carbon nanotubes is highly desired for their specific applications. By selecting different experimental conditions, we could selectively synthesize MWCNTs,[12] SWCNTs,[13] or DWCNTs[6] in the same CVD system. Furthermore, in this paper, we will show our effort to tune growth of DWCNTs with different diameter distributions which were determined by Raman scattering.

2. Experimental Section

The detailed experimental procedures for the preparation of DWCNTs with our method were described in detail elsewhere.[6] Typically, a two-stage furnace system fitted with a quartz tube was used. Ferrocene and sulfur powder were mixed uniformly and ground with mortar. The catalyst mixture was first sublimed in the first furnace, and then carried by the flowing argon and acetylene (C_2H_2) mixture into the second furnace. The grown DWCNTs in the second furnace were transported out of the reaction zone by the flowing gases and attached on the cooler part of the quartz tube inside wall.

The as-grown products could be easily peeled in large sheets. Typical transmission electron microscopy (TEM) images of

* Corresponding author. Tel: 86-01-82649081. Fax: 86-01-82640215. E-mail: ssxie@aphy.iphy.ac.cn.

† Current address: Lab of Mechanics of Soils, Structures and Materials, CNRS UMR 8579, Ecole Centrale Paris, 92295 Chatenay-Malabry, France. Phone: 33-1-41131508. Fax: 33-1-41131430. E-mail: Lci@mssmat.ecp.fr.

10.1021/jp026516h CCC: $25.00 © 2003 American Chemical Society
Published on Web 07/12/2003

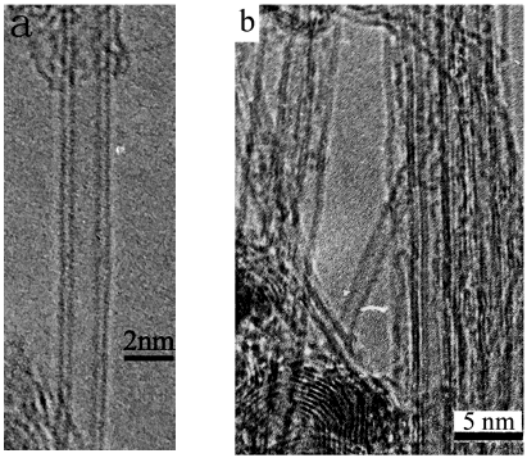

Figure 1. (a) HRTEM image of a single DWCNT; (b) HRTEM image of DWCNT bundles.

DWCNTs are displayed in Figure 1. Figure 1a shows a single DWCNT with the outer diameter of 1.86 nm and the inner diameter of 1.07 nm (measured by setting graphite {002} spacing (0.34 nm) as a reference). Figure 1b shows a DWCNT bundle and the double-walled feature is visible on the periphery of the bundle. We measured the diameter of DWCNTs from the HRTEM images, indicating outer tube diameters varied from 1.1 to 3.0 nm, and the inner tube diameters from 0.4 to 2.2 nm. That means the diameter range of our DWCNTs is similar to that of SWCNTs and may be well characterized by the Raman scattering.

The detailed characterization of the as-grown products prepared under different conditions was taken with a Renishaw microscopic confocal Raman spectrometer (RM2000) with 632.8 nm laser excitation wavelength. A 20× objective lens and a low laser power of ~0.8 kW/cm^2 were used to avoid sample heating. The spatial resolution of this Raman instrument is 1 cm^{-1}.

3. Results and Discussion

Typical Raman Spectra of DWCNTs. Figure 2 displays typical DWCNT micro-Raman spectra. Similar to that of the SWCNTs, the DWCNT Raman spectra in the range of 100−2000 cm^{-1} (in Figure 2a) also shows two "fingerprint" modes, that is, the tangential mode (TM) with a splitting peak (1594 and 1554 cm^{-1}) and the RBM in the lower frequency range. It is worth noting that the RBM frequencies of DWCNTs take a wider Raman frequency range (100−400 cm^{-1}) and display much richer peaks than that of SWCNTs (Figure 2b). A DWCNT can be considered as two coaxial SWCNTs coupled by van der Waals interaction. The interaction may lead to some mixed Raman vibrational modes.[5] However, we consider that the weak van der Waals interaction may not significantly affect the basic vibration of the outer and inner tubes compared with that of their SWCNT counterparts. Therefore, RBM Raman bands of DWCNTs can be identified according to the basic rules of that of SWCNTs. The RBM frequencies (ω_{RBM}, cm^{-1}) were found theoretically and experimentally to have a linear relationship with the diameter (d, nm) of SWCNTs and can be described as $\omega_{RBM} = 223.75/d$.[14] The wider RBM frequency range and the richer RBM peaks indicate that our DWCNTs have a wider inner and outer diameter distribution. Considering the thinnest inner diameter 0.4 nm and the interlayer spacing between the outer and the inner tube,[6,15] the RBM peaks higher than ~210 cm^{-1} might originate from the inner tubes. The lower frequency peaks might originate from both the outer tubes and the larger inner tubes.

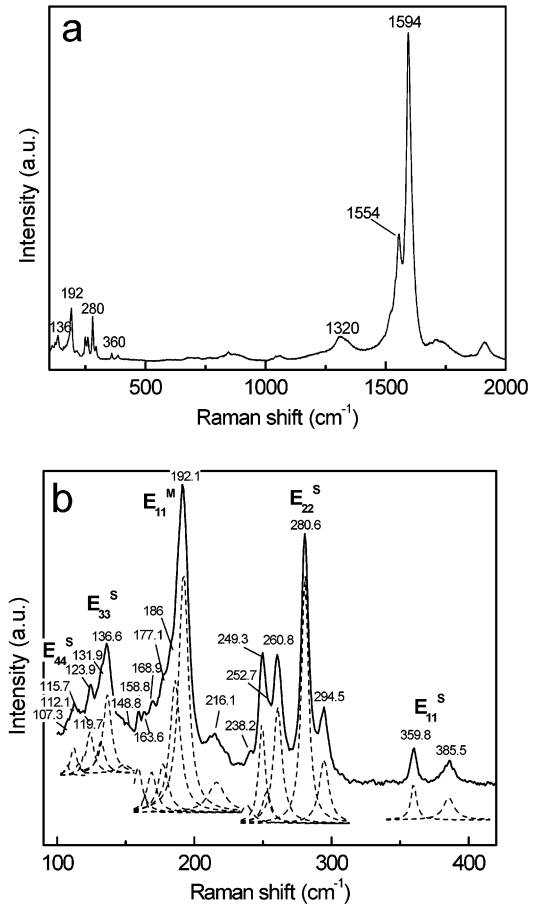

Figure 2. Typical DWCNT micro-Raman spectra. (a) Raman spectra in the range of 100−2000 cm^{-1} display two "fingerprint" features of TM and RBM bands; (b) high-resolution Raman spectra of RBM bands in (a).

Previous investigation indicated that RBM frequencies have a systematic upward shift for the SWCNTs in the bundles compared with the isolated ones due to the van der Waals interaction.[16−18] Here we assume that the influence of the van der Waals interaction between the outer and the inner tube in a DWCNT is the same as that in SWCNT bundles, and we can use the rule to assign the RBM frequencies to diameters of the outer and the inner tubes. That is, considering the interaction between the outer and the inner tube, the diameter dependence of the RBM frequency of DWCNTs can be fitted by the following equation:[17]

$$\omega_{RBM} = 238/d^{0.93} \quad (1)$$

To assign the RBM peaks to the two layers of DWCNTs, we first carried out the peak separations of the RBM bands using Lorentzian lines. The results are shown in Figure 2b with dashed lines. The two broad RBM bands located at the frequencies lower than 200 cm^{-1} are asymmetric with some obvious shoulders, and they are actually represented by a superposition of six or seven Lorentzian components with 4−18 cm^{-1} line width (fwhm). These components have small frequency intervals duo to the two-layer feature of DWCNTs (as shown in Figure 2b). On the other hand, RBM bands higher than 230 cm^{-1} seem more symmetric, and they can be separately simulated by a single Lorentzian line except for a small shoulder at 253.2 cm^{-1} (with 6−10 cm^{-1} line width). It indicates that the inner tubes with the smaller diameters have more discrete diameter distribution. Table 1 lists the peak positions and tube diameters of

TABLE 1: Possible Matches of Inner and Outer Tubes and Different Chirality Types of DWCNTs

exp. ω_{RBM}(cm^{-1}) and d_i (nm)for inner tubes	calcd. Δd [a] (nm)	calcd. ω_{RBM}(cm^{-1}) and d_o (nm) for outer tubes	exp. ω_{RBM}(cm^{-1}) and d_o (nm) for outer tubes	chirality pairs inner@outer
385.5(0.595)	0.837	170.4(1.432)	168.9(1.446)	S@M[b]
359.8(0.641)	0.833	165.9(1.474)	163.6(1.496)	S@M
294.5(0.795)	0.822	152.2(1.618)	158.8(1.545)	S@M
280.6(0.838)	0.820	148.8(1.657)	148.8(1.657)	S@S
260.8(0.906)	0.815	143.6(1.721)	148.8(1.657)	S@S
252.7(0.938)	0.813	141.4(1.751)	136.6(1.817)	S@S
249.3(0.951)	0.812	140.4(1.764)	136.6(1.817)	S@S
238.2(0.999)	0.809	137.2(1.808)	136.6(1.817)	S@S
216.1(1.109)	0.803	130.2(1.912)	131.9(1.886)	M@S
192.1(1.259)	0.795	121.9(2.054)	123.9(2.018)	M@S
186(1.304)	0.792	119.6(2.096)	119.7(2.094)	M@S
177.1(1.374)	0.789	116.2(2.163)	115.7(2.172)	M@S
168.9(1.446)	0.785	112.8(2.231)	112.1(2.247)	M@S
163.6(1.496)	0.783	110.6(2.279)	112.1(2.247)	M@S
158.8(1.545)	0.780	108.6(2.325)	107.3(2.355)	M@S
148.8(1.657)	0.775	104.1(2.432)	107.3(2.355)	S@S
136.6(1.817)	0.769	98.4(2.585)		
131.9(1.886)	0.766	96.1(2.652)		
123.9(2.018)	0.761	92.0(2.779)		
119.7(2.094)	0.758	89.8(2.852)		
115.7(2.172)	0.756	87.7(2.927)		
112.1(2.247)	0.753	85.7(3.000)		
107.3(2.355)	0.750	83.0(3.105)		

[a] Δd, the diameter difference between the outer and inner tube of a DWCNT which is determined by the equation $\Delta d = 0.688 + 0.2 \exp(-d_i/2)$.[19] [b] S and M denote semiconducting tube and metallic tube, respectively.

experimental and calculated data for the inner tubes and the outer ones. The possible match of an inner tube with an outer tube is according to the following rules. First, we assume that the interlayer spacing of a DWCNT is mainly determined by van der Waal interaction. It was revealed that the {002} spacing (d_{002}) of MWCNTs increases as the tube diameter decreases in the small diameter (<10 nm) region.[19] Our HRTEM observation and the previous report[11] indicated that DWCNTs with small diameters have the larger interlayer spacing than the average d_{002} spacing (0.34 nm) of MWCNTs. The diameter difference (Δd) between the outer tube and the inner tube of a DWCNT can be fitted by the empirical equation:[19]

$$\Delta d = 0.688 + 0.2 \exp(d_i/2) \text{ (nm)} \quad (2)$$

where d_i is the inner tube diameter. We set the experimentally observed peaks (the first column in Table 1) as those originate from the inner tubes. The diameters in the parentheses are determined by the relation (1). The diameter differences for the different DWCNTs are listed in the second column. Then, the diameters of the outer tubes are determined and the corresponding RBM bands are calculated (the third column). The experimental RBM bands are then correspond to the calculated ones with small variation (the fourth column).

Each SWCNT has a unique set of interband energies E_{ii} denoting the energy differences between the ith Van Hove singularities in the conduction and valence bands, and the interband energies have been found to depend both on the diameter and metallic or semiconducting character of the tubes.[7] Raman scattering by SWCNT has been experimentally shown to be a resonant process associated with this E_{ii}.[20] At a fixed laser energy (E_{laser}), a large enhancement in the Raman signal will occur when the $E_{ii} = E_{laser}$. From the diameter and chirality dependence of the interband energies,[21] we can conclude that the Raman spectra in Figure 2b fall in four resonant zones as label E_{33}^S, E_{11}^M, E_{22}^S, and E_{11}^S (where S and M denote semiconducting and metallic tube, respectively).

Theoretical calculation indicated that the structure of a DWCNT could be any chirality pairs of inner and outer layers, which suggests that any pair of DWCNTs, such as metallic−metallic, metallic−semiconducting, or semiconducting−semiconducting DWCNTs can be synthesized.[3] According to the possible match of coaxial inner and outer tubes in Table 1, we can determine the pair type of DWCNTs (listed in the fourth column). We find that three types of DWCNTs of S@S, S@M, and M@S (inner-tube@outer-tube) are identified, which suggests the theoretical results are correct. We should indicate that M@M type of DWCNTs should exist in the samples. However, the laser energy (1.96 eV) used here cannot resonantly excite metallic tubes in two diameter ranges simultaneously. By using different laser excitation energies, metallic tubes in different diameter ranges could be resonantly excited. For example, we can use 514.5 nm (2.41 eV) laser excitation to tune the second energy gap (E_{22}^M) of the metallic tubes with diameter of 1.9−2.0 nm, and use 632.8 nm (1.96 eV) laser excitation to tune E_{11}^M of metallic tubes with diameter of 1.1−1.3 nm, and the M@M type DWCNTs in these diameter range could be identified. Further detailed experiments and study are needed.

Tunable Growth of DWCNTs. As shown above, the DWCNTs can be well characterized by the Raman scattering, and it is very convenient to take an overview of the diameter distribution and chirality type of the as-grown DWCNTs. For tunable growth of DWCNTs, different experimental conditions were taken and the Micro-Raman scattering with 632.8 nm laser excitation was taken on the grown DWCNT samples. We found that the carbon partial pressure and the sulfur content had obvious influence on the diameter of the as-grown DWCNTs, while the reaction temperature (900−1150 °C) had little effect on the diameter distribution of the as-grown DWCNTs, though tube yield tended to increase at a higher reaction temperature. In the following section, we will show the Raman scattering results of DWCNTs prepared at the different carbon partial pressure and sulfur content. The results reported here might have some help to tunably grow different types of DWCNTs.

Figure 3 displays the Raman spectra of several samples prepared at different carbon partial pressure (with the buffer Ar flow rate of 1600 sccm). The evolution of the RBM bands in Figure 3a, i.e., the shift of RBM peaks toward higher

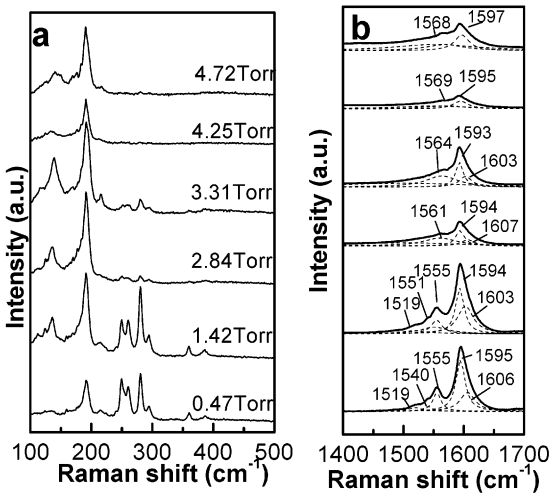

Figure 3. Raman spectra of DWCNTs prepared with different carbon partial pressure. (a) RBM bands; (b) TM bands.

frequency with decreasing carbon partial pressure, signals the increased production of smaller diameter DWCNTs. It indicates that DWCNTs produced at the lower carbon partial pressure have much smaller inner tubes. On the other hand, DWCNTs grown at the carbon partial pressure larger than 4.25 Torr have much larger diameters, and their RBM bands mainly center at a frequency lower than 200 cm^{-1}. Another "fingerprint" feature for the small diameter DWCNTs is that they have splitting peaks at the TM.[22−24] The splitting peak (W_G^-) is associated with vibrations along the circumferential direction, and it is strongly dependent on the tube diameter (d) and has a $-1/d^{1.4}$ relationship with the diameter.[23] That is, with the tube diameter decreasing, the W_G^- peak shifts down to a lower frequency. In Figure 3b, TM bands of DWCNTs produced at the lower carbon partial pressures of 0.47 Torr show obvious splitting peak at 1555 cm^{-1} with a shoulder at 1540 cm^{-1}. However, TM bands of DWCNTs produced at the higher carbon partial pressures of 3.31 Torr only show a shoulder at 1564 cm^{-1}. The evolution of the TM bands with different carbon partial pressure also verifies that the smaller DWCNTs easily grow at a lower carbon partial pressure.

The diameter dependence of the as-grown DWCNTs on the carbon partial pressure indicates that the growth process of DWCNTs is limited by the supply of carbon to the catalyst particles, especially at the lower carbon partial pressure. Nucleation of the large diameter DWCNTs might be limited at a lower carbon partial pressure, and the amount of the smaller DWCNTs in the resulting samples was increased.

Our previous experiments indicated that DWCNT growth is strongly dependent on the sulfur addition,[6] and only SWCNTs were produced without sulfur.[13] Addition of sulfur always increased the yield of SWCNTs in an arc discharge system[25] or a floating catalyst CVD system,[26] and the SWCNTs prepared with sulfur have much larger diameter. However, in our experimental condition for synthesizing DWCNTs, we could produce DWCNTs with much smaller inner diameters down to 0.4 nm.[6] Because the growth of DWCNT would be energetically more costly than that of SWCNT and the growth of smaller diameter tubes would have increased strain energy, we concluded that sulfur should alter the tube growth kinetics rather than thermodynamics. To further understand the role of sulfur, we prepared DWCNTs with different sulfur content, and the different samples were characterized using Raman scattering (in Figure 4).

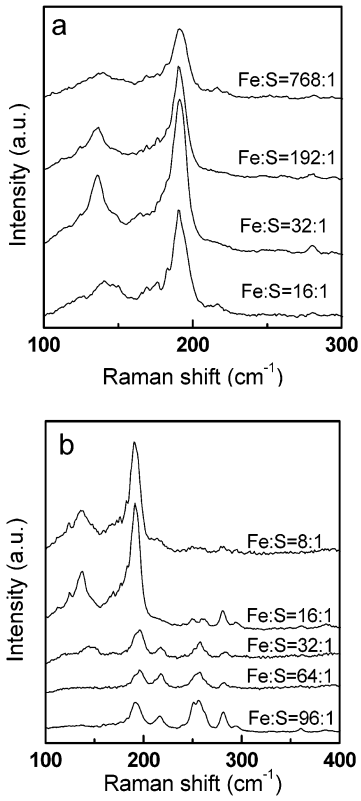

Figure 4. Raman RBM bands of DWCNTs prepared with different sulfur content at the carbon partial pressure: (a) 4.72 Torr, and (b) 2.84 Torr.

We found that the different sulfur content cannot alter the diameter distribution of DWCNTs at the higher carbon partial pressure. As shown in Figure 4a, at a carbon partial pressure of 4.72 Torr, we changed the sulfur content in a larger range, and there is hardly any variation in the RBM bands of resulting DWCNTs, though the yield of the products tended to slightly decrease with decreasing sulfur content. However, when the system is at a lower carbon partial pressure, we found that different content of sulfur could produce DWCNTs with different diameter feature. Figure 4b displays a set of Raman RMB bands of DWCNTs prepared at the carbon partial pressure of 2.84 Torr with different sulfur content. The evolution of the RBM bands indicates that more DWCNTs with smaller diameter could be produced by decreasing sulfur content.

The DWCNT diameter dependence on the sulfur content at different carbon partial pressure further proves that the carbon partial pressure is more important to tunable growth of DWCNTs. At the lower carbon partial pressure, as indicated above, the nucleation and growth of the DWCNTs are limited by the carbon supply, and only the more active catalyst particles can grow carbon nanotubes. When we decreased the sulfur content, the larger particles might become inactive due to reduced sulfur surface coverage.[6] On the other hand, those smaller particles retained their ability to grow carbon nanotubes. Therefore, the much smaller DWCNTs could tunably grow at the lower carbon partial pressure with the lower sulfur content.

4. Conclusion

In summary, DWCNTs prepared by the floating catalyst CVD method were characterized by Raman scattering. Compared with Raman spectra of SWCNTs, typical Raman RBM bands of

DWCNTs have much richer peaks since they could originate from both the inner tube and the outer tube. The possible match of the inner and outer tubes were assigned and their chirality types were discussed, and it is indicated that DWCNTs can be any chirality pairs. Raman scattering technique was demonstrated as a useful tool to characterize DWCNTs. Further understanding of Raman vibration of DWCNTs is still needed theoretically and experimentally.

Tunable growth of DWCNTs with different diameters was achieved in the floating catalyst system. We have found that DWCNTs with the smallest inner diameter of 0.4 nm could be synthesized,[6] The large curvature in the tube with the smaller diameter can dramatically change the electronic band structure, which makes these smallest carbon nanotubes have some novel quantum transport properties. Therefore, selective growth of this kind of DWCNTs may have great significance. Our further work will focus on the growth of the smallest DWCNTs and their transport measurement.

Acknowledgment. We thank F. E. Chen of Tsinghua University, P. R. China, for her assistance in Raman scattering work. This work is supported by National Natural Science Foundation of China and "973" National Key Basic Research Item-"Nanomaterials and Nanostructures".

References and Notes

(1) Iijiema, S. *Nature* (London) **1991**, *354*, 56.
(2) Iijima, S.; Ichihashi, T. *Nature* (London) **1993**, *364*, 603
(3) Saito, R.; Matsuo, R.; Kimura, T.; Dresselhaus, G.; Dresselhaus, M. S. *Chem. Phys. Lett*. **2001**, *348*, 187.
(4) Tanaka, K.; Aoki, H.; Ago, H.; Yamabe, T.; Okahara, K. *Carbon* **1997**, *35*, 121.
(5) Kwon, Y.; Tománek, D. *Phys. Rev. B* **1998**, *58*, R16001.
(6) Ci, L.; Rao, Z.; Zhou, Z.; Tang, D.; Yan, X.; Liang, Y.; Liu, D.; Yuan, H.; Zhou, W.; Wang, G.; Liu, W.; Xie, S. *Chem. Phys. Lett*. **2002**, *359*, 63.
(7) Rao, A. M.; Richter, E.; Bandow, S.; Chase, B.; Eklund, P. C.; Williams, K. A.; Fang, S.; Subbaswamy, K. R.; Menon, M.; Thess, A.; Smalley, R. E.; Dresselhaus, G.; Dresselhaus, M. S. *Science* **1997**, *275*, 187.
(8) Dresselhaus, M. S.; Eklund, P. C. *Adv. Phys*. **2000**, *49*, 705.
(9) Dresselhaus, M. S.; Dresselhaus, G.; Jorio, A.; Souza Filho, A. G.; Saito, R. *Carbon* **2002**, *40*, 2043.
(10) Bandow, S.; Takizawa, M.; Hirahara, K.; Yudasaka, M.; Iijima, S. *Chem. Phys. Lett*. **2001**, *337*, 48.
(11) Hutchison, J. L.; Kiselev, N. A.; Krinichnaya, E. P.; Krestinin, A. V.; Loutfy, R. O.; Morawsky, A. P.; Muradyan, V. E.; Obraztsova, E. D.; Sloan, J.; Terekhov, S. V.; Zakharov, D. N. *Carbon* **2001**, *39*, 761.
(12) Ci, L.; Wei, J.; Wei, B.; Liang, J.; Xu, C.; Wu, D. *Carbon* **2001**, *39*, 329.
(13) Ci, L.; Xie, S.; Tang, D.; Yan, X.; Li, Y.; Liu, Z.; Zou, X.; Zhou W.; Wang, G. *Chem. Phys. Lett.* **2001**, *349*, 191.
(14) Bandow, S.; Asaka, S. *Phys. Rev. Lett*. **1998**, *80*, 3779.
(15) Qin, L. C.; Zhao, X. L.; Hirahara, K.; Miyamoto, Y.; Ando, Y.; Iijima, S. *Nature* (London) **2000**, *408*, 50.
(16) Henrard, L.; Hernández, E.; Bernier, P.; Rubio, A. *Phys. Rev. B* **1999**, *60*, R8521.
(17) Rols, S.; Righi, A.; Alvarez, L.; Anglaret, E.; Almairac, R.; Journet, C.; Bernier, P.; Sauvajol, J. L.; Benito, A. M.; Maser, W. K.; Muñoz, E.; Martinez, M. T.; de la Fuente, G. F.; Girard, A.; Ameline, J. C. *Eur. Phys. J. B* **2000**, *18*, 201.
(18) Rao, A. M.; Chen, J.; Richter, E.; Schlecht, U.; Eklund, P. C.; Haddon, R. C.; Venkateswaran, U. D.; Kwon, Y.-K.; Tománek, D. *Phys. Rev. Lett*. **2001**, *86*, 3895.
(19) Kiang, C.-H.; Endo, M.; Ajayan, P. M.; Dresselhaus, G.; Dresselhaus, M. S. *Phys. Rev. Lett.* **1998**, *81*, 1869.
(20) Pimenta, M. A.; Marucci, A.; Brown, S. D. M.; Matthews, M. J.; Rao, A. M.; Eklund, P. C.; Smalley, R. E.; Dresselhaus, G.; Dresselhaus, M. S. *J. Mater. Res*. **1998**, *13*, 2396.
(21) Kataura, H.; Kumazawa, Y.; Maniwa, Y.; Umezu, I.; Suzuki, S.; Ohtsuka, Y.; Achiba, Y. *Synth. Met*. **1999**, *103*, 2555.
(22) Kasuya, A.; Sasaki, Y.; Saito, Y.; Tohji, K.; Nishina, Y. *Phys. Rev. Lett.* **1997**, *78*, 4434.
(23) Jorio, A.; Pimenta, M. A.; Souza Filho, A. G.; Samsonidze, Ge. G.; Swan, A. K.; Ünlü, M. S.; Goldberg, B. B.; Saito, R.; Dresselhaus, G.; Dresselhaus, M. S. *Phys. Rev. Lett*. **2003**, *90*, 107403.
(24) Dubay, O.; Kresse, G.; Kuzmany, H. *Phys. Rev. Lett*. **2002**, *88*, 235506.
(25) Kiang, Ch.; Goddard, W. A., III; Beyers, R.; Salem, J. R.; Bethune, D. S. *J. Phys. Chem.* **1994**, *98*, 6612.
(26) Cheng, H. M.; Li, F.; Su, G.; Pan, H. Y.; He, L. L.; Sun, X.; Dresselhaus, M. S. *Appl. Phys. Lett*. **1998**, *72*, 3243.